Cp*); 1.2-2.2 m (66 H, PCy_3); -10.38 d (6 H, hydrides, J_{PH} = 14.5 Hz).

X-ray Data Collection, Structure Determination, and Refinement for $\{Cp^*Ru[(C_6H_9)P(C_6H_{11})_2]\}BF_4 \cdot CH_3CH_2OH$ (4) and $\{[Cp^*RuH[P(C_6H_{11})_3](\mu\text{-}H)_2(CuCl)\}_2$ (6). Crystals of 4 were obtained by recrystallization from ethanol and those of 6 by recrystallization from toluene/hexane.

The crystallographic data are summarized in Table III. Unit cell parameters were obtained from least-squares refinements of 62 (4) and 50 (6) carefully centered reflections in the 2θ range 20-35°. Data were corrected for Lorentz and polarization effects. Absorption corrections were also applied to the data on the basis of a series of ψ scans for 4 and by using the method of Walker and Stewart[26] for (6).

Both structures were solved by Patterson and difference Fourier techniques and refined by full-matrix least squares first with isotropic and then with anisotropic thermal parameters for non-hydrogen atoms not involved in disorder. In 4, the fluoride groups of the BF_4^- anion were found disordered around the B atom, but no simple way of modeling this disorder was obtained and, eventually, only the four more intense peaks around boron were used in the refinement. Additionally, a disordered ethanol molecule was also present in the crystal structure of 4 and only the three highest peaks were included to account for this crystallization molecule. For 6, one of the cyclohexyl rings bonded to the P atom was observed distributed in two positions, C(23)-C(28) and C(23)'-C(28)', with refining occupancy factors of 0.708 (8) and 0.292 (8), respectively. Hydrogen atoms for 4 were placed at idealized positions and included in the last cycles of refinement riding on carbon atoms with a fixed thermal parameter. Carbon-bonded hydrogen atoms (except those of the disordered C_9H_{11} ring) were found in difference Fourier maps for 6 and refined riding on carbon atoms with a common thermal parameter. The three hydrides present in 6 were clearly found and were refined as normal isotropic atoms. The last cycles of refinement were carried out on the basis of 308 and 298 variables for 4 and 6, respectively. Unit weights were used in the first stages of the refinement, and then a weighting scheme, $w = K[\sigma^2(F_o) + gF_o^2]^{-1}$, was used, with K = 1.000 and g = 0.004 50 for 4 and K = 1.234 and g = 0.0005 for 6. The analytical scattering factors, corrected for the real and imaginary parts of anomalous dispersions, were taken from ref 27.

All calculations used the SHELX76 package[28] run on a VAX 11/780 computer. Tables IV and V collect the atomic coordinates for both complexes. Additional crystallographic data are available as supplementary material.

Acknowledgment. F.A.J. and A.O. are grateful to the Comision Interministeriel de Ciencia y Tecnologia (CICYT; Grant No. PPB 86-0101) and the Subdireccion General de Cooperacion Internacional for financial support. T.A., B.C., F.A.J., and A.O. thank "Action Intêgrêe France-Espagne".

Supplementary Material Available: For both structures, tables of anisotropic temperature factors, hydrogen coordinates, full experimental details for X-ray analysis, complete bond lengths and angles, and least-squares planes (28 pages); lists of structure factors (45 pages). Ordering information is given on any current masthead page.

(26) Walker, N.; Stewart, D. *Acta Crystallogr., Sect. A: Found. Crystallogr.* **1983**, *A39*, 1581.

(27) *International Tables for X-ray Crystallography*; Kynoch: Birmingham, England, 1974; Vol. IV.

(28) Sheldrick, G. M. SHELX76, Program for Crystal Structure Determination; University of Cambridge: Cambridge, England, 1976.

Organometallic Salts with Large Second-Harmonic-Generation Powder Efficiencies: (*E*)-1-Ferrocenyl-2-(1-methyl-4-pyridiniumyl)ethylene Salts

Seth R. Marder,* Joseph W. Perry, and Bruce G. Tiemann

Jet Propulsion Laboratory, California Institute of Technology, Pasadena, California 91109

William P. Schaefer

Division of Chemistry and Chemical Engineering,† California Institute of Technology, Pasadena, California 91125

Received August 22, 1990

A series of salts of the form (E)-$(\eta\text{-}C_5H_5)Fe(\eta\text{-}C_5H_4)CH{=}CH(4\text{-}C_5H_4N\text{-}1\text{-}CH_3)^+X^-$ has been synthesized. Variation of the counterion leads to materials with second-harmonic-generation powder efficiencies at 1907-nm fundamental as large as 220 times that of a urea reference standard. This is the largest value reported for an organometallic compound. The crystal structure of the nitrate salt, which had a powder SHG efficiency 110 times that of urea, was determined: $(FeC_{18}H_{18}N)^+NO_3^-$, monoclinic, *Cc* (No. 9), a = 17.618 (4) Å, b = 10.780 (3) Å, c = 12.528 (3) Å, β = 133.18 (2)°, Z = 4.

Introduction

There is currently considerable interest in the synthesis of new materials with large second-order optical nonlinearities.[1] The induced polarization of a molecule by an electric field is given by the power series

$$\rho(E) = \alpha \cdot \mathbf{E} + \beta \cdot\cdot \mathbf{EE} + \gamma \cdot\cdot\cdot \mathbf{EEE} + \ldots \quad (1)$$

Second-order nonlinear optical effects including second-harmonic generation (SHG) and the linear electrooptical effect, both of which are technologically significant, arise from the first hyperpolarizability, β. It is

† Contribution No. 8197.

0276-7333/91/2310-1896$02.50/0

generally accepted that large molecular second-order nonlinearities are associated with structures that have a large difference between ground- and excited-state dipole moments as well as a large transition dipole moment.[1,2] Noncentrosymmetric molecules with π donor–acceptor interactions are promising candidates to fulfill these requirements.

The polarization experienced by a *material* in the presence of an electric field is expressed by a similar power series

$$P(E) = \chi^{(1)}\cdot\mathbf{E} + \chi^{(2)}\cdot\cdot\mathbf{EE} + \chi^{(3)}\cdot\cdot\cdot\mathbf{EEE} + \ldots \quad (2)$$

in which $\chi^{(2)}$ is analogous to β; however, it accounts for local field effects, which are consequences of the surrounding medium. Just as it is a necessary criterion for molecules to be noncentrosymmetric if β is to be nonzero, likewise the bulk material must be noncentrosymmetric for $\chi^{(2)}$ to be nonzero. Since bulk nonlinear susceptibilities are strongly dependent on crystal structure and molecular orientation, approaches permitting the facile modification of crystallographic phase while conserving units with large hyperpolarizability are of considerable interest. One such approach based on organic salts has been demonstrated[3] with the organic cation (*E*)-1-(4-(dimethylamino)-phenyl)-2-(1-methyl-4-pyridiniumyl)ethylene (1). This cation was crystallized with a variety of counterions, and the powder SHG efficiencies showed a dramatic variation, with the largest value being found for the methanesulfonate salt. In fact, the powder SHG efficiency of this salt is some 30 times that of *m*-nitroaniline (or about 220 times that of urea) for a 1907-nm fundamental, the largest value reported until recently.[4] We have recently extended this methodology to a variety of organic chromophores and were able to isolate several materials with powder efficiencies in excess of 200 times that of urea.[5]

In contrast to the extensive studies of organic materials for nonlinear optics, to date the nonlinear optical properties of organometallic compounds have received little attention.[6] Some organometallic groups are expected to be excellent donors or acceptors since they are among the strongest oxidants or reductants known. Furthermore, the diversity of metal oxidation states and the ability to systematically vary the ligand environment around the metal[7] might provide a versatile means for optimizing the hyperpolarizability, β, or the crystallographic factors that control the bulk susceptibility. Recently, a powder SHG efficiency of 62 times that of urea was reported for the ferrocene-based compound (*Z*)-1-ferrocenyl-2-(4-nitrophenyl)ethylene (2), demonstrating that organometallic compounds could exhibit large second-order nonlinear susceptibilities.[8a] Electric-field-induced SHG studies of 2 and related compounds indicate that compounds of this class have large molecular hyperpolarizabilities as well.[8b] Here we present results of an investigation of organometallic salts for second-order nonlinear optics.

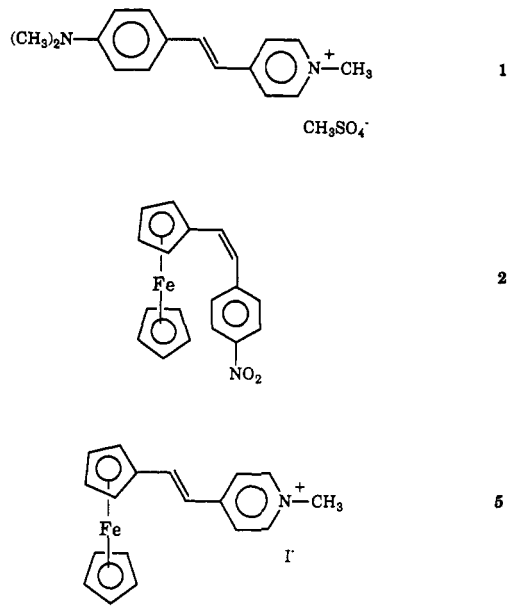

Figure 1. Structures of organometallic and organic compounds with large powder SHG efficiencies.

Results and Discussion

In this paper we report the synthesis and powder SHG efficiencies of a series of new organometallic salts that incorporate the ferrocenyl and ruthenocenyl moieties as the donors and 1-methylpyridinium as the acceptor connected by a CH=CH linkage (see Figure 1). These cations have been crystallized with a range of anions of varying size and shape, and their powder SHG efficiencies have been determined. Powder SHG efficiences comparable to that of (1)methanesulfonate have been attained and are the largest reported for organometallic compounds.

Reaction of (η-C_5H_5)Fe(η-C_5H_4CHO) (3) with (4-CH_3-C_5H_4N-1-CH_3)I ((4)I) in methanol in the presence of piperidine at 60 °C for 4 h under argon yielded, after filtration and precipitation with ether, the new compound (*E*)-1-ferrocenyl-2-(1-methyl-4-pyridiniumyl)ethylene iodide ((5)I), in 96% yield. In this manner compound (5)I can readily be prepared on a 5–10-g scale. The compounds (5)CF_3SO_3 and (5)(*p*-$CH_3C_6H_4SO_3$) were prepared by direct reaction of (4)CF_3SO_3, and (4)(*p*-$CH_3C_6H_4SO_3$) with 3. The compounds (5)Br and (5)Cl were prepared by metathesis of (5)CF_3SO_3 with (n-C_4H_9)$_4$NBr or (n-C_4H_9)$_4$NCl, respectively, in acetone. Compound (5)Cl is readily soluble in water; thus, addition of $NaBF_4$, $NaB(C_6H_5)_4$, KPF_6, and $NaNO_3$ to aqueous solutions of (5)Cl yielded (5)BF_4, (5)-$B(C_6H_5)_4$, (5)PF_6, and (5)NO_3 as precipitates that were isolated, washed with water, and recrystallized from acetone–ether. The formulations are supported by ^{1}H NMR spectra and elemental analyses (see Experimental Section).

Since it should be possible to vary the energy of the charge-transfer band by varying the metal, we synthesized

(1) See, for example: (a) Williams, D. J. *Angew. Chem., Int. Ed. Engl.* **1984**, *23*, 690. (b) *Nonlinear Optical Properties of Organic and Polymeric Materials*; Williams, D. J., Ed.; ACS Symposium Series 233; American Chemical Society: Washington, DC, 1983. (c) *Nonlinear Optical Properties of Organic Molecules and Crystals*; Chemla, D. S., Zyss, J., Eds.; Academic Press: Orlando, FL, 1987; Vol. 1 and 2.

(2) (a) Oudar, J. L.; Chemla, D. S. *J. Chem. Phys.* **1977**, *66*, 2664. (b) Levine, B. F.; Bethea, C. G. *J. Chem. Phys.* **1977**, *66*, 1070. (c) Lalama, S. J.; Garito, A. F. *Phys. Rev. A* **1979**, *20*, 1179.

(3) Meredith, G. In ref 2b, p 27.

(4) (a) Tam, W.; Wang, Y.; Calabrese, J. C.; Clement, R. A. Nonlinear Optical Properties of Organic Materials. Proc. SPIE-*Int. Soc. Opt. Eng.* **1988**, *971*, 107. (b) Perry, J. W.; Stiegman, A. E.; Marder, S. R.; Coulter, D. R.; Beratan, D. N.; Brinza, D. E.; Klavetter, F. L.; Grubbs, R. H. *Proc. SPIE-Int. Soc. Opt. Eng.* **1988**, *971*.

(5) Marder, S. R.; Perry, J. W.; Schaefer, W. P. *Science* **1989**, *245*, 626.

(6) (a) Frazier, C. C.; Harvey, M. A.; Cockerham, M. P.; Chauchard, E. A.; Lee, C. H. *J. Phys. Chem.* **1986**, *90*, 5703. (b) Eaton, D. F.; Anderson, A. G.; Tam, W.; Yang, Y. *J. Am. Chem. Soc.* **1987**, *109*, 1886. (c) Calabrese, J. C.; Tam, W. *Chem. Phys. Lett.* **1987**, *133*, 245.

(7) (a) Geoffroy, G. L.; Wrighton, M. S. *Organometallic Photochemistry*; Academic Press: New York, 1979. (b) Collman, J. P.; Hegedus, L. S. *Principles and Applications of Organotransition Metal Chemistry*, 2nd ed.; University Science Books: Mill Valley, CA, 1987.

(8) (a) Green, M. L. H.; Marder, S. R.; Thompson, M. E.; Bandy, J. A.; Bloor, D.; Kolinsky, P. V.; Jones, R. J. *Nature* **1987**, *330*, 360. (b) Cheng, L.-T.; Tam, W.; Meredith, G. R.; Marder, S. R. *Mol. Cryst. Liq. Cryst.* **1990**, *189*, 137.

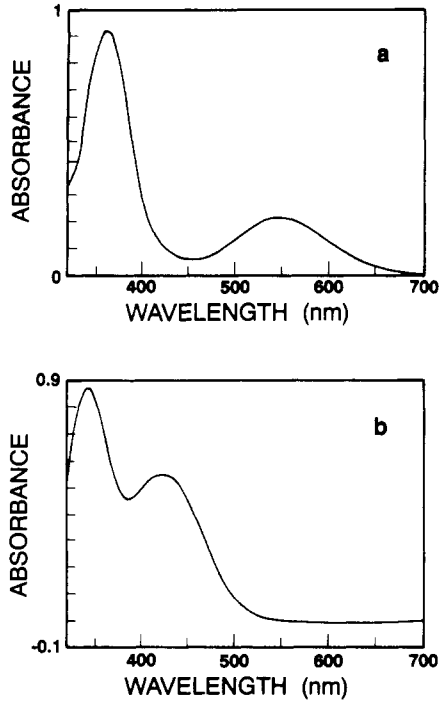

Figure 2. UV-visible spectra of (a) (*E*)-1-ferrocenyl-2-(1-methyl-4-pyridiniumyl)ethylene triflate and (b) (*E*)-1-ruthenocenyl-2-(1-methyl-4-pyridiniumyl)ethylene triflate in acetonitrile.

Table I. Powder SHG Efficiencies of (E)-$(\eta$-$C_5H_5)Fe(\eta$-$C_5H_4)CH{=}CH(4$-C_5H_4N-1-$CH_3)^+X^-$ Salts

anion	SHG value[a]	color	anion	SHG value[a]	color
I^-	220	purple	$B(C_6H_5)_4^-$	13	purple
Br^-	165	purple	PF_6^-	0.05	purple
Cl^-	0	purple	$CF_3SO_3^-$	0	purple
BF_4^-	50	purple	p-$CH_3C_6H_4SO_3^-$	13	burgundy
NO_3^-	120	purple			

[a] Second-harmonic intensity measured with use of 1907-nm fundamental radiation. Values reported are relative to a urea reference sample (53–104-μm particle size). SHG values less than 0.02 times that of urea are set to 0.

the (*E*)-1-ruthenocenyl-2-(1-methyl-4-pyridiniumyl)-ethylene cation as the iodide ((**6**)I), triflate ((**6**)CF_3SO_3), and tosylate ((**6**)(p-$CH_3C_6H_4SO_3$)) salts. We expected that the larger ligand field splitting of the ruthenium d orbitals as compared to that of the iron d orbitals would move the charge-transfer band to higher energy. The visible absorption spectrum of (**5**)I in solution exhibits two strong low-lying bands (acetonitrile) at λ_{max} = 362 nm (ϵ = 28 200 cm^{-1} M^{-1}) and λ_{max} = 551 nm (ϵ = 6700 cm^{-1} M^{-1}) (Figure 2a), which are attributed to charge-transfer transitions[9] (identical results were obtained for (**5**)CF_3SO_3). In contrast, the ruthenium analogue has bands at λ_{max} = 354 nm (ϵ = 21 500 cm^{-1} M^{-1}) and (λ_{max} = 432 nm (ϵ = 11 700 cm^{-1} M^{-1}) (Figure 2b), consistent with our expectations. Interestingly, the colors of the ruthenium salts varied in the solid state. Thus, (**6**)(p-$CH_3C_6H_4SO_3$) was yellow, (**6**)CF_3SO_3 was orange, and (**6**)I was burgundy, indicating the importance of packing effects on the linear as well as the nonlinear optical properties of these materials.

In order to determine whether counterion variation could be used to modify crystallographic packing so as to realize the potentially large second-order susceptibilities for this class of organometallic salts, we examined their

(9) Marder, S. R.; Cheng, L. T.; Tam, W.; Calabrese, J. C.; Green, J. C. Submitted for publication.

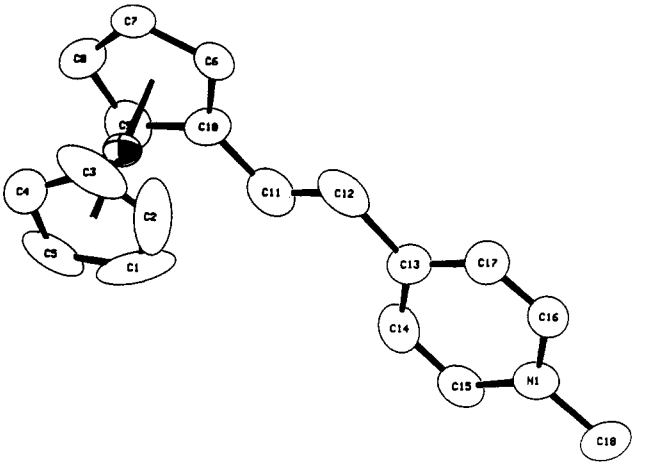

Figure 3. ORTEP drawing of the (*E*)-1-ferrocenyl-2-(1-methyl-4-pyridiniumyl)ethylene cation with atomic numbering (hydrogen atoms omitted for clarity).

powder SHG efficiencies. The powder SHG efficiencies varied as a function of counterion shape and size (Table I). In the iron series the salts with halides I^- and Br^- gave large signals, whereas the smaller Cl^- ion resulted in an SHG-inactive material that is probably centrosymmetric. As discussed by Meredith,[3] Coulombic interactions between counterions (the Madelung energy) in salt crystals can give an overwhelming stabilization of alignments that would otherwise be unfavorable. It is noted that various samples of (**5**)I gave SHG signals which varied from 125 to 240 times that of the urea reference. SHG intensity as a function of particle size will reach a maximum, drop slightly, and level off for a phase-matchable material; in contrast, if a material is not phase-matchable, the SHG intensity will reach a peak value and then decrease to a small value. Qualitatively, we observed that smaller crystals gave a larger powder efficiency, suggesting that the material is not phase-matchable at this frequency.[10] Nonetheless, the large powder efficiency implies large components of the $\chi^{(2)}$ susceptibility that could lead to large electrooptic coefficients.[11]

In contrast to the relatively large powder SHG values observed for the ferrocene salts, the ruthenium values were small; only (**6**)(p-$CH_3C_6H_4SO_3$) gave an appreciable signal, the same as that of urea (SH at 532 nm). The compounds in this study are ionic, precluding solution EFISH study measurements; solutions of the salts will undoubtedly be conductive. However, consistent with the notion that the less electron rich ruthenium will be a less effective donor than will iron, solution EFISH studies of neutral ruthenium metallocenes gave β values roughly 0.6 of those for the analogous iron metallocenes.[8b,9] Therefore, differences in molecular hyperpolarizability of the iron versus ruthenium salts alone cannot account for the order of magnitude differences in observed SHG values. Furthermore, since the iron salts were measured with 1907-nm fundamental radiation and the ruthenium salts with 1064-nm fundamental radiation, given the color of the materials, effects due to resonant/dispersive enhancement should, if anything, tend to enhance the observed values of the ruthenium salts. It seems likely, therefore, that the compounds

(10) Kurtz, S. K.; Perry, T. T. *J. Appl. Phys.* **1968**, *39*, 3798.

(11) For a detailed analysis of the relationship between the various components of the hyperpolarizability tensor β_{ijk} and the macroscopic nonlinear coefficients $\chi^{(2)}_{ijk}$ see: (a) Chemla, D. S.; Oudar, J. L.; Jerphagnon, J. *Phys. Rev. B* **1975**, *12*, 4534. (b) Zyss, J.; Oudar, J. L. *Phys. Rev.* A **1982**, *26*, 2028. (c) Oudar, J. L.; Zyss, J. *Phys. Rev. A* **1982**, *26*, 2016.

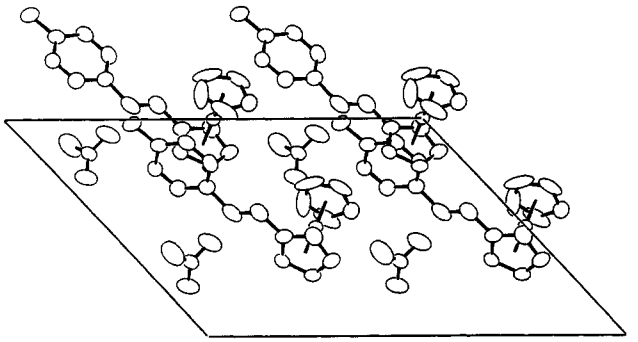

Figure 4. Packing diagram of (*E*)-1-ferrocenyl-2-(1-methyl-4-pyridiniumyl)ethylene nitrate: view roughly along the ***b*** axis.

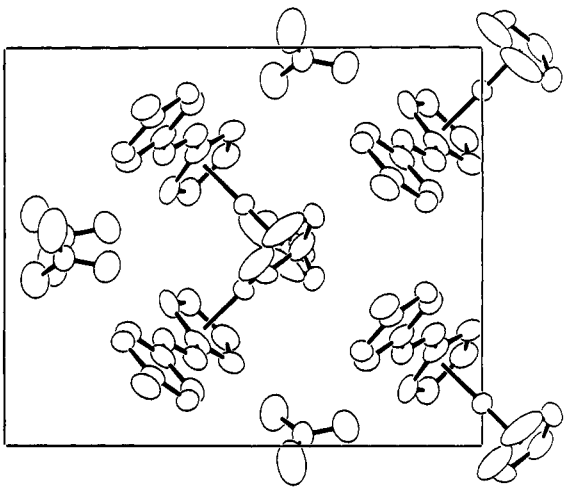

Figure 5. Packing diagram of (*E*)-1-ferrocenyl-2-(1-methyl-4-pyridiniumyl)ethylene nitrate: view roughly along the *a* axis.

examined here crystallize in centrosymmetric space groups or with nearly centrosymmetric orientations. Why the ruthenium compounds would pack so differently from their iron analogues, despite the fact that, to a first approximation, they are geometrically very similar, remains an unanswered question.

The crystal structure of (5)NO_3 was determined; the compound crystallizes in the noncentrosymmetric monoclinic space group *Cc*. Distances and angles are generally as expected, save for a short (1.234 (17) Å) C11–C12 double bond. Details are in the supplementary material. An ORTEP drawing of the cation is shown in Figure 3, and packing diagrams are shown in Figures 4 and 5. Figure 4 illustrates the excellent alignment of the chromophores, which is largely responsible for the large powder SHG efficiency of (5)NO_3. The ions pack in the cell with the Fe···N1 vector aligned approximately along the *c* axis at an angle to it of 25.7° and with an angle of 34.9° between the Fe···N1 vectors related by *Cc* symmetry. Selected bond lengths and angles are given in Table II and atomic parameters in Table III.

Since the first hyperpolarizability is a tensor as is $\chi^{(2)}$, it is important to realize that the three-dimensional ferrocene molecules are qualitatively different from most of the effectively two-dimensional organic chromophores which have been examined in the past. Thus, in addition to charge transfer from the cyclopentadienyl (Cp) ring to the pyridine ring there may be orthogonal iron to Cp charge transfer. So whereas the Cp to N1 vectors are almost parallel, which is desirable for electrooptic switching, the Fe to Cp vectors are almost orthogonal, which is more optimal for phase-matched harmonic generation.[11]

Table II. Selected Bond Lengths and Bond Angles for (*E*)-(η-C_5H_5)Fe(η-C_5H_4)CH=CH(4-C_5H_4N-1-CH_3)$^+NO_3^-$

Distances (Å)			
Fe–Cp1	1.639	N1–C18	1.476 (14)
Fe–Cp2	1.638	N2–O1	1.134 (19)
C10–C11	1.493 (16)	N2–O2	1.177 (14)
C11–C12	1.234 (17)	N2–O3	1.179 (15)
C12–C13	1.580 (16)		
Angles (deg)			
Cp2–Fe–Cp1	178.7	C17–C13–C12	116.1 (10)
C11–C10–C6	129.2 (10)	C17–C13–C14	115.6 (11)
C11–C10–C9	121.4 (10)	O2–N2–O1	112.2 (12)
C12–C11–C10	121.3 (11)	O3–N2–O1	123.1 (13)
C13–C12–C11	120.6 (11)	O3–N2–O2	124.1 (11)
C14–C13–C12	128.3 (10)		

Table III. Final Atomic Parameters (×10⁴) for (*E*)-(η-C_5H_5)Fe(η-C_5H_4)CH=CH(4-C_5H_4N-1-CH_3)$^+NO_3^-$

atom	*x*	*y*	*z*	U_{eq},[a] Å²
Fe	0	1072 (0.7)	0	772 (2)
C1	−826 (21)	438 (22)	−2004 (13)	2248 (76)
C2	−262 (16)	−415 (21)	−1132 (32)	2235 (75)
C3	−453 (10)	−685 (8)	−384 (17)	1799 (46)
C4	−1214 (9)	22 (13)	−738 (13)	1298 (30)
C5	−1470 (8)	795 (11)	−1796 (17)	1514 (45)
C6	1561 (6)	1434 (10)	1551 (10)	1083 (24)
C7	1151 (7)	1391 (11)	2217 (9)	1100 (24)
C8	381 (8)	2287 (9)	1554 (10)	1182 (25)
C9	257 (8)	2908 (7)	427 (11)	1225 (31)
C10	969 (7)	2409 (8)	426 (8)	1102 (23)
C11	1018 (8)	2799 (8)	−669 (11)	1259 (27)
C12	1672 (7)	2359 (9)	−656 (12)	1340 (30)
C13	1693 (7)	2758 (8)	−1849 (9)	1045 (21)
C14	1081 (7)	3622 (10)	−2945 (13)	1211 (28)
C15	1179 (6)	3855 (7)	−3908 (10)	1058 (22)
N1	1904 (5)	3247 (5)	−3790 (6)	961 (16)
C16	2526 (7)	2382 (7)	−2702 (10)	942 (19)
C17	2413 (8)	2157 (8)	−1794 (11)	1074 (24)
C18	2051 (8)	3504 (9)	−4796 (9)	1224 (25)
N2	3761 (5)	282 (7)	6588 (8)	1080 (20)
O1	4001 (9)	−424 (16)	6195 (14)	2827 (56)
O2	2863 (7)	498 (9)	5694 (10)	1895 (33)
O3	4363 (7)	834 (11)	7696 (9)	1919 (37)

[a] $U_{eq} = {}^1/_3\sum_i\sum_j[U_{ij}(a^*_i a^*_j)(\vec{a}_i\cdot\vec{a}_j)]$.

Summary

In this paper we have demonstrated that organometallic salts can have large powder SHG efficiencies, comparable to some of the largest powder SHG efficiencies of organic materials. In addition, it was shown that the substitution of ruthenium for iron leads to smaller powder efficiencies. This work also demonstrates that the salt methodology, which has been successfully used for planar organic chromophores, can also be used with three-dimensional organometallic compounds.

Experimental Section

General Considerations. All manipulations of air- and/or moisture-sensitive compounds were carried out with use of standard Schlenk- or vacuum-line techniques with argon as the flush gas.

Reagent grade methanol, acetone, diethyl ether, and dichloromethane were purchased from Fisher Scientific. Methyl tosylate (97%), piperidine (99%), methyl triflate, methyl iodide and sodium tetrafluoroborate were obtained from Aldrich Chemical Co. and were used without purification. Tetrabutylammonium chloride hydrate (97%) was obtained from Fluka Chemie and was used without purification. 4-Picoline (98%) was obtained from Mallinckrodt Chemical Co. and was used without purification. [$^2H_6$]acetone (99.9% ^2H) was obtained from Cambridge Isotope Laboratories, and [^2H]chloroform (99.9% ^2H) was obtained from Aldrich Chemical Co.; both were used without

purification. The 1-methyl-4-picolinium triflate, tosylate, and iodide salts were prepared by reaction of picoline with the appropriate alkylating reagent in dichloromethane, followed by precipitation with diethyl ether and isolation by filtration. The white crystalline materials were used without further purification. $(\eta\text{-}C_5H_5)Ru(\eta\text{-}C_5H_4CHO)$ (**7**) was prepared by the literature procedure.[12]

^1H NMR spectra were recorded on a Bruker AM-500 spectrometer. Chemical shifts were referenced to the chemical shift of the residual protons of the solvent with respect to tetramethylsilane. UV–visible spectra were recorded on a Hewlett-Packard 8154A diode array spectrophotometer. Elemental analyses were performed by the California Institute of Technology Analytical Facility or by Galbraith Analytical Laboratories.

Synthesis. (*E*)-1-Ferrocenyl-2-(1-methyl-4-pyridiniumyl)ethylene Iodide. The reaction of $(\eta\text{-}C_5H_5)Fe(\eta\text{-}C_5H_4CHO)$ (**3**) with $(1\text{-}CH_3C_5H_4N\text{-}4\text{-}CH_3)I$ ((**4**)I) in methanol in the presence of piperidine at 60 °C for 4 h under argon yielded, after filtration and precipitation with diethyl ether, (*E*)-1-ferrocenyl-2-(1-methyl-4-pyridiniumyl)ethylene iodide ((**5**)I; 2.04 g, 96% yield). In this manner the triflate and tosylate salts were also prepared. ^1H NMR of (**5**)I (in $CDCl_3$): δ 8.85 (d, J = 6.6 Hz, 2 H, CHN), 7.82 (d, J = 6.8 Hz, 2 H, *CH*CHN), 7.66 (d, J = 15.6 Hz, 1 H, $(\eta\text{-}C_5H_4)CH$), 6.66 (d, J = 15.8 Hz, 1 H, $(\eta\text{-}C_5H_4)CHCH$), 4.63, 4.58 (each t, J = 1.8 Hz, 2 H, $\eta\text{-}C_5H_4$), 4.43 (s, 3 H, CH_3), 4.20 (s, 5 H, $\eta\text{-}C_5H_5$).

Representative Procedures for Synthesis of Various Salts by Metathesis of Counterions. (a) Conversion of Triflate Salt to Chloride Salt by Metathesis. Tetrabutylammonium chloride (wet, 0.2 M) in acetone was added dropwise with stirring to a nearly saturated solution of the triflate salt in acetone, yielding a precipitate. The addition was continued until an additional drop afforded no more precipitate. The precipitate was isolated by filtration, washed with acetone, and dried. In this manner the bromide salt was prepared.

(b) Conversion of Chloride Salt to Tetrafluoroborate Salt by Metathesis. A saturated aqueous solution of sodium tetrafluoroborate was added dropwise with stirring to a nearly saturated aqueous solution of the chloride salt, yielding a precipitate. The addition was continued until an additional drop afforded no more precipitate. The precipitate was isolated by filtration, washed with water, and dried. The material was purified by recrystallization from acetone–diethyl ether. In this manner the tetraphenylborate, hexafluorophosphate, and nitrate salts were prepared.

Analytical Data for (*E*)-1-Ferrocenyl-2-(1-methyl-4-pyridiniumyl)ethylene Salts. Triflate. Anal. Calcd for $C_{19}H_{18}F_3FeNO_3S$: C, 50.35; H, 4.00; N, 3.09. Found: C, 50.43; H, 3.80; N, 3.17.

BF_4. Anal. Calcd for $C_{18}H_{18}BF_4FeN$: C, 55.30; H, 4.63; N, 3.58. Found: C, 55.47; H, 4.73; N, 3.76.

Tosylate. Anal. Calcd for $C_{25}H_{25}FeNO_3S$: C, 63.17; H, 5.30; N, 2.94. Found: C, 62.95; H, 5.45; N, 2.80.

Cl. Anal. Calcd for $C_{18}H_{18}ClFeN\cdot H_2O$: C, 60.45; H, 5.64; N, 3.92. Found: C, 59.82; H, 5.49; N, 3.94.

I. Anal. Calcd for $C_{18}H_{18}FeIN$: C, 50.15; H, 4.20; N, 3.24. Found: C, 49.96; H, 3.89; N, 3.36.

Br. Anal. Calcd for $C_{18}H_{18}BrFeN$: C, 56.29; H, 4.71; N, 3.89. Found: C, 55.95; H, 5.16; N, 3.60.

PF_6. Anal. Calcd for $C_{18}H_{18}F_6FeNP$: C, 48.14; H, 4.04; N, 3.12. Found: C, 48.35; H, 4.03; N, 2.98.

$B(C_6H_5)_4$. Anal. Calcd for $C_{42}H_{38}BFeN$: C, 80.92; H, 6.14; N, 2.25. Found: C, 81.06; H, 6.10; N, 2.13.

NO_3. Anal. Calcd for $C_{18}H_{18}FeN_2O_3$: C, 59.04; H, 4.95; N, 7.65. Found: C, 57.68; H, 5.04; N, 7.52.

(*E*)-1-Ruthenocenyl-2-(1-methyl-4-pyridiniumyl)ethylene Triflate. Reaction of $(\eta\text{-}C_5H_5)Ru(\eta\text{-}C_5H_4CHO)$ (**7**; 0.613 g, 2.37 mmol) with $(1\text{-}CH_3C_5H_4N\text{-}4\text{-}CH_3)CF_3SO_3$ ((**4**)CF_3SO_3; 0.474 g, 1.84 mmol) in methanol (15 mL) in the presence of piperidine (~1 mL) at 60 °C for 4 h under argon yielded, after filtration and precipitation with diethyl ether, the new compound (*E*)-1-ruthenocenyl-2-(1-methyl-4-pyridiniumyl)ethylene triflate ((**6**)CF_3SO_3; 0.718 g, 78% yield). In this manner the iodide and tosylate salts were isolated in 72% and 18% yields, respectively. ^1H NMR of (**6**)CF_3SO_3 (in $(CD_3)_2CO$): δ 8.78 (d, J = 6.7 Hz, 2 H, CHN), 8.07 (d, J = 6.8 Hz, 2 H, *CH*CHN), 7.81 (d, J = 15.9 Hz, 1 H, $(\eta\text{-}C_5H_4)CH$), 6.97 (d, J = 16.0 Hz, 1 H, $(\eta\text{-}C_5H_4)CHCH$), 5.10, 4.82 (each t, J = 1.8 Hz, 2 H, $\eta\text{-}C_5H_4$) 4.58 (s, 5 H, $\eta\text{-}C_5H_5$), 4.42 (s, 3 H, CH_3).

Table IV. Crystallographic Data for $(E)\text{-}(\eta\text{-}C_5H_5)Fe(\eta\text{-}C_5H_4)CH{=}CH(4\text{-}C_5H_4N\text{-}1\text{-}CH_3)^+NO_3^-$

formula: $(FeC_{18}H_{18}N)^+NO_3^-$	fw: 366.20
V = 1735.0 (10) Å^3	space group: *Cc* (No. 9)
a = 17.618 (4) Å	T = 23 °C
b = 10.780 (3) Å	λ = 0.71073 Å
c = 12.528 (3) Å	ρ_{calc} = 1.40 (1) g cm^{-3}
β = 133.18 (2)°	μ = 9.10 cm^{-1}
Z = 4	$R(F_o)$ = 0.0466
	GOF = 3.51

Analytical Data for (*E*)-1-Ruthenocenyl-2-(1-methyl-4-pyridiniumyl)ethylene Salts. Triflate. Anal. Calcd for $C_{19}H_{18}F_3NO_3SRu$: C, 45.78; H, 3.64; N, 2.81. Found: C, 45.95; H, 3.76; N, 2.89.

Tosylate. Anal. Calcd for $C_{25}H_{25}NO_3SRu$: C, 57.68; H, 4.84; N, 2.69. Found: C, 57.50; H, 4.96; N, 2.77.

I. Anal. Calcd for $C_{18}H_{18}INRu$: C, 45.39; H, 3.81; N, 2.94. Found: C, 45.45; H, 3.86; N, 3.10.

Powder SHG Measurements. Powder SHG efficiencies were determined with use of the 1064-nm output of a Q-switched Nd:YAG laser. Absorption of the SH by the dark colored salts was avoided by using 1907-nm light (SH at 953.5 nm) obtained by Raman shifting (first Stokes line of H_2) the 1064-nm output of a Q-switched Nd:YAG laser. The powder SHG measurements were made with use of a modification of the Kurtz powder method.[9] A dual-beam system (with a urea sample in the reference arm) was used to normalize the SH signals for laser shot-to-shot fluctuations. Pulse energies used were in the range of 100–500 μJ with spot sizes of 2–3 mm. The diffusely backscattered SH signals were collected and isolated with use of filters and a monochromator and detected with use of photomultiplier tubes (Hamamatsu R406) whose outputs were amplified and integrated by using 10-ns gate widths. Samples were ground unsized microcrystalline powders; particle sizes were estimated to span from about 40 to 150 μm. Given the typically broad ranges of sizes and the possibility of preferential orientation of particles in assembly of the samples, the uncertainties in the measured efficiencies can be quite large, perhaps a factor of 2 or more.

Crystal Structure Determination. A small irregular chunk of (**5**)NO_3 was cut from a larger crystal and glued to a glass fiber with epoxy cement. The crystal was centered on the diffractometer, and a preliminary cell and orientation matrix were obtained. The data were collected in a triclinic cell with a = 10.325 (3) Å, b = 10.609 (2) Å, c = 10.780 (3) Å, α = 59.47 (2)°, β = 58.55 (3)° and γ = 73.50 (2)°. These final dimensions were obtained from 25 reflections with 34° < 2θ < 38°. The cell was transformed to a *C*-centered monoclinic cell (an *I*-centered cell with $\beta \approx 92°$ could also have been used); the data were corrected for a small, isotropic decay, and they were placed on an approximately absolute scale by Wilson's method. A Patterson map gave the position of the iron atom; the vectors in the map, the number of formula units in the cell, and the Wilson statistics all suggested the noncentrosymmetric space group *Cc*. Crystallographic data are presented in Table IV. A Fourier map phased only on the iron atom did not reveal the rest of the molecule, but several atoms were identified, and successive structure factor-Fourier cycles gave the final model. Least-squares refinements were slow: even after heavy atoms were anisotropic and all hydrogen atoms had been introduced (on the basis of a Fourier map for C18 and at calculated positions, C–H = 0.95 Å, for the remainder), it took 16 cycles of full-matrix refinement to converge. The maximum shift/esd in the final cycle was 0.03 for B(11) of C12; the maximum excursions in the final difference map were +0.46 (near C11 and C12) and −0.24 e Å^{-3}.

Calculations were done with programs of the CRYM crystallographic computing system and ORTEP. The data were averaged in point group 2/*m*, and refinements were carried out with F'' being ignored for Fe (0.845 electron). Scattering factors and correction for anomalous scattering were taken from ref 13. R

(12) Hofer, O.; Schogl, K. *J. Organomet. Chem.* **1968**, *13*, 443.

$= \sum||F_o| - |F_c||/\sum F_o$, for $F_o^2 > 0$, and the goodness of fit is equal to $[\sum w(F_o^2 - F_c^2)^2/(n = p)]^{1/2}$, where n is the number of data and p is the number of parameters refined. The variances of the individual reflections were assigned on the basis of counting statistics plus an additional term, $0.0141I^2$. Variances of the merged reflections were determined by standard propagation of error plus another additional term, $0.014I^2$.

Acknowledgment. The research described in this paper was performed by the Jet Propulsion Laboratory, California Institute of Technology, as part of its Center for Space Microelectronics Technology, which is supported by the Strategic Defense Initiative Organization, Innovative Science and Technology Office, through an agreement with the National Aeronautics and Space Administration. S.R.M. thanks Professor Robert Grubbs for access to synthetic facilities at Caltech. We thank Richard E. Marsh for his persistence in finding the correct structure in the initial Fourier map. The diffractometer used in this study was purchased with a grant from the National Science Foundation (No. CHE-8219039). We thank Paul Groves and Kelly Perry for technical assistance.

Supplementary Material Available: An ORTEP drawing of the cation with atom numbering and tables of crystal data, final parameters of all the atoms, and complete distances and angles (6 pages); a table of observed and calculated structure factors (7 pages). Ordering information is given on any current masthead page.

(13) *International Tables for X-Ray Crystallography*; Kynoch Press: Birmingham, England 1974; Vol. IV, pp 71, 149.

Diphenylphosphide Derivatives of Dineopentylgallium and -Indium. Crystal and Molecular Structures of $[(Me_3CCH_2)_2GaPPh_2]_2$ and $[(Me_3CCH_2)_2InPPh_2]_3$

Michael A. Banks, O. T. Beachley, Jr.,* Lisa A. Buttrey, Melvyn Rowen Churchill,* and James C. Fettinger

Department of Chemistry, State University of New York at Buffalo, Buffalo, New York 14214

Received October 30, 1990

The two compounds $(Me_3CCH_2)_2MPPh_2$ (M = Ga, In) have been prepared by metathetical reactions between $(Me_3CCH_2)_2MCl$ and $KPPh_2$ and fully characterized. The characterization data include elemental analyses (C, H), melting points, IR and ^1H and ^{31}P NMR spectral studies, cryoscopic molecular weight studies in benzene solution, and single-crystal X-ray structural studies. The gallium compound exists as a dimer in benzene solution and in the solid state. The corresponding indium derivative exists as a monomer–dimer equilibrium mixture in benzene solution and as a trimer in the solid state. Thus, $(Me_3CCH_2)_2InPPh_2$ represents an unusual example of an amphoteric compound that exhibits three different degrees of association. $[(Me_3CCH_2)_2GaPPh_2]_2$ crystallizes in the monoclinic space group $P2_1/n$ (No. 14) with a = 11.076 (3) Å, b = 18.996 (3) Å, c = 21.753 (5) Å, β = 100.128 (9)°, V = 4505 (2) Å^3, and Z = 4 (dimeric molecules). The molecule contains a buckled Ga_2P_2 core (dihedral angles of 142.2° across P(1)···P(2) and 145.6° across Ga(1)···Ga(2)); Ga–P distances are in the range 2.479 (3)–2.512 (3) Å, and Ga–C(neopentyl) bond lengths are in the range 1.996 (12)–2.016 (12) Å. $[(Me_3CCH_2)_2InPPh_2]_3$ crystallizes in the rhombohedral space group $R\bar{3}$ (No. 148); unit cell parameters (hexagonal setting) are a = 20.873 (5) Å, c = 29.037 (4) Å, V = 10956 (4) Å^3, and Z = 6 (trimeric molecules). The molecules lie on sites of C_3 symmetry, their In_3P_3 cores having a chair conformation. The independent In–P distances are 2.677 (1) and 2.699 (2) Å; In–C(neopentyl) bond lengths are 2.182 (6) and 2.210 (7) Å.

Introduction

The formation of group 13–15 materials such as GaAs and InP from single-source precursors of the type $R_2MER'_2$ (M = group 13 element, E = group 15 element)[1] has provided the motivation to understand more fully the chemistry of this class of compounds. Since the most desirable compounds for preparing group 13–group 15 materials by organometallic chemical vapor deposition (OMCVD) are volatile liquids, our goal has been to study the factors that control the degree of association of these Lewis amphoteric species, their structures, and their physical properties. Some representative examples of monomers are $(C_5Me_5)_2GaAs(SiMe_3)_2$[2] and t-$Bu_2GaAsBu^t_2$,[3] those of dimers are $(Me_2GaPBu^t_2)_2$,[4] $(Me_2InPBu^t_2)_2$,[5] and $[(Me_3SiCH_2)_2InPPh_2]_2$,[6] and those of trimers are $(Et_2GaPEt_2)_3$[7] and $[Cl_2GaAs(CH_2SiMe_3)_2]_3$.[8] These examples might suggest that steric effects provide an important factor for controlling the degree of association. However, other factors[9] including valency angle strain,

(1) Cowley, A. H.; Jones, R. A. *Angew. Chem., Int. Ed. Engl.* **1989**, *28*, 1208 and references therein.
(2) Byrne, E. K.; Parkanyi, L.; Theopold, K. H. *Science (Washington, D.C.)* **1988**, *241*, 332.
(3) Higa, K. T.; George, C. *Organometallics* **1990**, *9*, 275.
(4) (a) Arif, A. M.; Benac, B. L.; Cowley, A. H.; Geerts, R. L.; Jones, R. A.; Kidd, K. B.; Power, J. M.; Schwab, S. T. *J. Chem. Soc., Chem. Commun.* **1986**, 1543. (b) Arif, A. M.; Benac, B. L.; Cowley, A. H.; Jones, R. A.; Kidd, K. B.; Nunn, C. M. *New J. Chem.* **1988**, *12*, 553.
(5) Aitchison, K. A.; Backer-Dirks, J. D. J.; Bradley, D. C.; Faktor, M. M.; Frigo, D. M.; Hursthouse, M. B.; Hussain, B.; Short, R. L. *J. Organomet. Chem.* **1989**, *366*, 11.
(6) Beachley, O. T., Jr.; Kopasz, J. P.; Zhang, H.; Hunter, W. E.; Atwood, J. L. *J. Organomet. Chem.* **1987**, *325*, 69.
(7) (a) Maury, F.; Constant, G. *Polyhedron* **1984**, *3*, 581. (b) Maury, F.; Combes, M.; Constant, G.; Cartes, R.; Renucci, J. B. *J. Phys., Colloq.* **1982**, *43*, C1.
(8) Pitt, C. G.; Purdy, A. P.; Higa, K. T.; Wells, R. L. *Organometallics* **1986**, *5*, 1266.
(9) Beachley, O. T., Jr.; Coates, G. E. *J. Chem. Soc.* **1965**, 3241.

0276-7333/91/2310-1901$02.50/0